arXiv:math-ph/0410001v1 1 Oct 2004

Elastic energy of liquid crystals in convex polyhedra

A Majumdar[†] [‡], JM Robbins[†] & M Zyskin[†] [*]
School of Mathematics
University of Bristol, University Walk, Bristol BS8 1TW, UK
and
Hewlett-Packard Laboratories,
Filton Road, Stoke Gifford, Bristol BS12 6QZ, UK

January 29, 2022

Abstract

We consider nematic liquid crystals in a bounded, convex polyhedron described by a director field $\mathbf{n}(\mathbf{r})$ subject to tangent boundary conditions. We derive lower bounds for the one-constant elastic energy in terms of topological invariants. For a right rectangular prism and a large class of topologies, we derive upper bounds by introducing test configurations constructed from local conformal solutions of the Euler-Lagrange equation. The ratio of the upper and lower bounds depends only on the aspect ratios of the prism. As the aspect ratio is varied, the minimum-energy conformal state undergoes a sharp transition from being smooth to having singularities on the edges.

[*]a.majumdar@bristol.ac.uk, j.robbins@bristol.ac.uk, m.zyskin@bristol.ac.uk

The continuum theory of liquid crystals [1] is a prototypical nonlinear field theory in which topological considerations play a fundamental role [2, 3, 4], both in equilibrium (eg [5, 6]) and dynamical phenomena (eg [7]). Nematic liquid crystals are represented by a director field $\mathbf{n}(\mathbf{r})$, which describes the mean local orientation of the constituent rod-like molecules. In confined geometries, boundary conditions, which depend on the properties of the substrate, can play a significant role (see, eg [8]).

In this Letter, we consider director fields in a bounded, three-dimensional convex polyhedron P. While natural theoretically, the problem also has a technological motivation; polyhedral geometries have been proposed as a mechanism for engendering bistability in liquid crystal display cells [9], [10]. Polyhedral cells can support two (or more) energetically stable director configurations with contrasting optical properties. Power is required only to switch pixel states but not to maintain them. Bistable cells offer the promise of displays with higher resolution and requiring less power than is available with current technologies based on monostable cells.

We suppose P has strong azimuthal anchoring, so that $\mathbf{n}$ satisfies *tangent boundary conditions* – on the faces of P, $\mathbf{n}$ must be tangent to the faces. Tangent boundary conditions imply that, on the edges of P, $\mathbf{n}$ is parallel to the edges, and, therefore, is necessarily discontinuous at the vertices. We restrict our study to configurations which are continuous everywhere else, ie as continuous as possible. As P is simply connected, we can then regard $\mathbf{n}(\mathbf{r})$ as a unit-vector field, rather than a director field. We obtain lower bounds for the elastic energy of $\mathbf{n}$ in terms of its topological invariants, and, for a rectangular prism, upper bounds, which differ from the lower bounds only by a geometry-dependent factor. The upper bounds are obtained from local conformal solutions of the Euler-Lagrange equation, whose energetics indicate the onset of edge singularities as the prism becomes cubic.

It turns out that tangent boundary conditions produce a large family of topologically distinct configurations. A complete classification is given in Ref. [11], whose results we briefly summarise. Tangent unit-vector fields on P can be classified up to homotopy (ie, continuous deformations) by a family of invariants: the *edge orientations*, *kink numbers* and *trapped areas*. The edge orientations are just the values of $\mathbf{n}$ on the edges of P, and therefore are essentially signs. The kink numbers determine the number of times $\mathbf{n}$ winds along an (outward-oriented) path on a face of P which joins a pair of adjacent edges. On such a path, the initial and final values of $\mathbf{n}$ are determined by the edge orientations; in between, $\mathbf{n}$ describes a curve on the circle of unit vectors tangent to the face. The shortest curve between the endpoints is assigned kink number 0. In general, the kink numbers are integers. The trapped areas, Ω^a, are defined as follows. Let C^a be a surface inside P which

separates the vertex a from the other vertices. Then Ω^a is the area of the region $\mathbf{n}(C^a)$ on the unit two-sphere. This may be written as $\int_{C^a} \mathbf{D} \cdot \mathbf{dS}$, where $\mathbf{dS}$ is the outward-oriented area element on C^a, and

$$D_j = \tfrac{1}{2}\epsilon_{jkl}(\partial_k \mathbf{n} \times \partial_l \mathbf{n}) \cdot \mathbf{n}. \tag{1}$$

$\mathbf{D}$ may be regarded as the vector field dual to the pull-back, $\mathbf{n}^*\omega$, of the outward-oriented area form ω on the sphere (in polar coordinates, $\omega = \sin\theta\, d\theta \wedge d\phi$). Ω^a is independent of the choice of C^a, and may be thought of as the degree of a fractional point defect at a. Ω^a need not be integral, but the allowed values of Ω^a for given edge orientations and kink numbers differ by integer multiples of 4π (complete coverings of the sphere). These integers are the wrapping numbers. The invariants satisfy certain sum rules, which follow from the fact that $\mathbf{n}$ is continuous away from the vertices. The sum of the kink numbers on each face is determined by the edge orientations, while the trapped areas sum to zero. All values of the invariants consistent with the sum rules can be realised, and two configurations are homotopic if and only if their invariants are the same.

In the continuum theory, the energy of $\mathbf{n}$ is given by the elastic, or Frank-Oseen, energy [1],

$$E = \int_P \big[K_1(\operatorname{div}\mathbf{n})^2 + K_2(\mathbf{n}\cdot\operatorname{\mathbf{curl}}\mathbf{n})^2 + K_3(\mathbf{n}\times\operatorname{\mathbf{curl}}\mathbf{n})^2 + K_4 \operatorname{div}\left((\mathbf{n}\cdot\nabla)\mathbf{n} - (\operatorname{div}\mathbf{n})\mathbf{n}\right)\big]\, dV. \tag{2}$$

Tangent boundary conditions imply that the contribution from the K_4-term, which is a pure divergence, vanishes. In the so-called one-constant approximation, the remaining elastic constants K_1, K_2 and K_3 are taken to be the same. In this case, (2) simplifies to

$$E = K\int_P (\nabla\mathbf{n})^2\, dV = K\int_P \sum_{j=1}^{3} (\partial_j \mathbf{n})^2\, dV. \tag{3}$$

Stable (or quasi-stable) configurations are minima (or local minima) of the energy. In the one-constant approximation, local minimisers satisfy the Euler-Lagrange equation and boundary conditions

$$\begin{aligned} \Delta\mathbf{n} &= (\mathbf{n}\cdot\Delta\mathbf{n})\mathbf{n}, \\ (\mathbf{c}\cdot\mathbf{n})_{\partial P} &= (\mathbf{c}\times\nabla_c\mathbf{n})_{\partial P} = 0, \end{aligned} \tag{4}$$

where $\mathbf{c}$ is the outward unit-normal on the boundary ∂P of P, and ∇_c denotes the derivative along $\mathbf{c}$ (the normal derivative here); the condition on $\nabla_c\mathbf{n}$

ensures there is no boundary contribution to the first-order variation of the elastic energy. (Minimisers of the energy (3) are called *harmonic maps* in the mathematics literature.)

Our first result is a lower bound for the energy (3) in each homotopy class. The derivation extends an argument from a seminal paper of Brezis, Coron and Lieb [5] to the polyhedral boundary-value problem we are considering here. Below we restrict to the case where $\nabla\mathbf{n}$ is smooth away from the vertices. In fact, the bound is good provided only that $\nabla\mathbf{n}$ is square-integrable [12].

Since $\mathbf{n}$ is normalised, the partial derivatives $\partial_j\mathbf{n}$, $j = 1, 2, 3$, are orthogonal to $\mathbf{n}$, and therefore are linearly dependent. Thus, at each point $\mathbf{r}$, there is at least one direction, $\mathbf{w}$ say, in which the derivative of $\mathbf{n}$ vanishes. Let us introduce unit vectors $\mathbf{u}$ and $\mathbf{v}$ which together with $\mathbf{w}$ define an orthonormal frame. Then

$$(\nabla\mathbf{n})^2 = (\nabla_u\mathbf{n})^2 + (\nabla_v\mathbf{n})^2 \geq 2|\nabla_u\mathbf{n} \times \nabla_v\mathbf{n}|, \tag{5}$$

where equality holds if and only if $\nabla_u\mathbf{n}$ and $\nabla_v\mathbf{n}$ are orthogonal and of equal length. From (1), the right-hand side of (5) is just $2|(\mathbf{u} \times \mathbf{v}) \cdot \mathbf{D}|$, which in turn is just equal to $2|\mathbf{D}|$, since, by inspection, $\mathbf{D}$ is orthogonal to $\mathbf{u}$ and $\mathbf{v}$. Then

$$(\nabla\mathbf{n})^2 \geq 2|\mathbf{D}|. \tag{6}$$

Let $\xi(\mathbf{r})$ be a continuous scalar function with piecewise continuous gradient such that $|\nabla\xi| = 1$. Then $|\mathbf{D}| \geq \mathbf{D} \cdot \nabla\xi$. Let $\hat{P}$ be a domain obtained by excising from P vanishingly small neighborhoods of each vertex. From (3) and (6), it follows that

$$E \geq 2K \int_{\hat{P}} \mathbf{D} \cdot \nabla\xi \, dV. \tag{7}$$

But $\mathbf{D}$ has zero divergence, as follows from the fact that area-form ω is closed (as well as from direct calculation). Integrating by parts, we get

$$E \geq 2K \oint_{\partial\hat{P}} \xi\mathbf{D} \cdot \mathbf{dS}. \tag{8}$$

The boundary of $\hat{P}$, denoted $\partial\hat{P}$, consists of (parts of) the faces of P as well as the boundaries of the excised regions. But $\mathbf{D}$ vanishes on the faces of $\hat{P}$, as tangent boundary conditions imply that the tangential derivatives of $\mathbf{n}$ are parallel to each other there. On the boundaries of the excised regions, ξ can be set to its values ξ^a at the vertices. Thus, the integral $\int_{\partial\hat{P}} \xi\mathbf{D} \cdot \mathbf{dS}$

reduces to a weighted sum of fluxes of $\mathbf{D}$ through the excised boundaries. These fluxes are just the trapped areas. We obtain the lower bound

$$E \geq 2K \sum_a \xi^a \Omega^a. \tag{9}$$

To proceed, note the values ξ^a are constrained; since $|\nabla \xi| = 1$, we must have $|\xi^a - \xi^b| \leq L^{ab}$, where L^{ab} is the length of the edge between vertices a and b. Conversely, given a set of values ξ^a satisfying these inequalities, we can construct a function $\xi(\mathbf{r})$ which interpolates between these values, and for which $\nabla \xi$ is piecewise continuous with unit norm (for example, let $\xi(\mathbf{r}) = \max_a(\xi^a - |\mathbf{r} - \mathbf{a}|)$). Therefore, we can express the lower bound (9) in terms of the trapped areas and the lengths of the edges of P,

$$E \geq 2K \max_{\xi^a : |\xi^a - \xi^b| \leq L^{ab}} \sum_a \xi^a \Omega^a. \tag{10}$$

(10) specifies a linear optimisation problem, which can be solved by standard methods.

We note that because $\sum_a \Omega^a = 0$, the optimal solution ξ^a is in general only determined up to an overall additive constant. If the one-constant approximation is dropped, K in (10) can be replaced by the smallest of the three elastic constants K_1, K_2 and K_3.

Next, we consider the case where P is a right rectangular prism, with sides of length $L_x \geq L_y \geq L_z$. Moreover, within P, we consider configurations (and their homotopy classes) which are *reflection-symmetric* about the mid-planes of P. That is,

$$\mathbf{n}(L_x - x, y, z) = \mathbf{n}(x, L_y - y, z) = \mathbf{n}(x, y, L_z - z) = \mathbf{n}(x, y, z) \tag{11}$$

(we plan to treat more general geometries and homotopy classes in the future). Clearly, a reflection-symmetric configuration is determined by its values in the octant of the prism, denoted $R = \{0 \leq r_j \leq \frac{1}{2} L_j\}$, as are its invariants. In particular, the trapped areas at two vertices are either the same or differ by a sign according to whether the vertices are related by an even or odd number of reflections. Let Ω^0 denote the trapped area at the origin. Taking ξ^a in (10) (optimally) to be L_z or 0 according to whether Ω^a is $|\Omega^0|$ or $-|\Omega^0|$, we obtain the explicit lower bound $E \geq E_-$, where

$$E_- = 8KL_z|\Omega^0|. \tag{12}$$

In the remainder of this Letter, we introduce a family of reflection-symmetric configurations which are local solutions of the Euler-Lagrange

equation (4). From these we infer upper bounds for the energy as well as the onset of edge singularities as the geometry is varied.

Candidates for low-energy configurations are those for which (6) becomes an equality. This is so if, on R, $\mathbf{n}$ is radially constant (ie, $\mathbf{n}(\lambda\mathbf{r}) = \mathbf{n}(\mathbf{r})$) and conformal. Here, conformal means that the map $\mathbf{t} \mapsto \nabla_t \mathbf{n}(\mathbf{r})$ from vectors $\mathbf{t}$ orthogonal to $\hat{\mathbf{r}}$ to vectors $\nabla_t \mathbf{n}(\mathbf{r})$ orthogonal to $\mathbf{n}(\mathbf{r})$ preserves orientation, angles and ratios of lengths (or else vanishes). If $\mathbf{n}$ is radially constant then $\mathbf{D}$ is radial (cf (1)), while if $\mathbf{n}$ is also conformal, $\mathbf{D} = \frac{1}{2}(\nabla\mathbf{n})^2\hat{\mathbf{r}}$. It is straightforward to verify that radially constant, conformal configurations satisfy (4) in R (but fail to on the mid-planes of P, where the normal derivatives of $\mathbf{n}$ are discontinuous).

Suppose $\mathbf{n}$ is a reflection-symmetric configuration which is radially constant and conformal in R (below we will show how to construct such configurations). Then, from (3), and using reflection symmetry, we get

$$E = 8K \int_R (\nabla\mathbf{n})^2 dV = 16K \int_R \hat{\mathbf{r}} \cdot \mathbf{D} dV = 16K \int_{\partial R} r\mathbf{D} \cdot \mathbf{dS}, \qquad (13)$$

where we have used $\nabla \cdot \mathbf{D} = 0$. We obtain an upper bound E_+ for E by replacing r by its maximum value on ∂R, namely $\frac{1}{2}(L_x^2 + L_y^2 + L_z^2)^{1/2}$. The integral which remains is just the flux of $\mathbf{D}$ through R. As tangent boundary conditions imply there is no contribution from the exterior faces of R (ie, $x = 0$, $y = 0$ or $z = 0$), this just gives the trapped area. Thus

$$E_+ = 8K(L_x^2 + L_y^2 + L_z^2)^{1/2}|\Omega^0|. \qquad (14)$$

Like E_-, E_+ is proportional to $|\Omega^0|$, and $E_+/E_- = (a_{xz}^2 + a_{yz}^2 + 1)^{1/2}$, where $a_{ij} = L_i/L_j$ denote the aspect ratios of the prism. For the cube, this ratio is $\sqrt{3}$.

It remains to construct radially constant, conformal configurations $\mathbf{n}(\mathbf{r})$ in R satisfying tangent boundary conditions. For this, it is convenient to introduce the stereographic projection $(e_x, e_y, e_z) \mapsto (e_x + ie_y)/(1 + e_z)$ from the sphere to the extended complex plane $\mathbb{C}^e$. Projecting both $\mathbf{r}$ and $\mathbf{n}$, we obtain a complex-valued function $f(w)$ of complex argument w given by

$$\left(\frac{n_x + in_y}{1 + n_z}\right)(x, y, z) = f\left(\frac{x + iy}{r + z}\right). \qquad (15)$$

The domain of f is the stereographic image of R, which is the quarter-disc Q given by $|w| \leq 1$ and $\operatorname{Re} w$, $\operatorname{Im} w \geq 0$. $\mathbf{n}$ conformal is equivalent to f locally analytic.

The form of f is determined by tangent boundary conditions. Under stereographic projection, the xz-face is mapped to the real w-axis, so we

require that i) $f(w)$ is real if w is real. Similarly, the yz- and xy-faces are mapped to the imaginary axis and the unit circle respectively, so we require that ii) $f(w)$ is imaginary if w is imaginary, and iii) $|f(w)| = 1$ if $|w| = 1$. To proceed, we assume that f has a meromorphic extension from Q to $\mathbb{C}^e$. Then the conditions i)–iii) may be continued to the following functional equations:

$$\bar{f}(w) = f(w), \tag{16a}$$

$$\bar{f}(-w) = -f(w), \tag{16b}$$

$$f(w)\bar{f}(1/w) = 1. \tag{16c}$$

Together, (16a) and (16c) imply that $f(w)f(1/w) = 1$, which in turn implies that if w is a zero of f, then $1/w$ is a pole. f meromorphic implies the number of zeros and poles in the unit disk must be finite (otherwise there would be an accumulation of one or the other). It follows that f has only a finite number of zeros and poles in $\mathbb{C}^e$, so that f is rational.

(16b) and (16c) imply that, if w is a zero of f, then so are $\bar{w}$ and $-w$, and similarly if w is a pole. One can then show that every reciprocal pair $(w, 1/w)$ of zeros and poles has a unique representative in Q. For convenience, we divide these representatives into three groups: the strictly real $r_1, \ldots, r_a$, with $0 < r_j < 1$ (as (16c) rules out zeros and poles of modulus one); the strictly imaginary $is_1, \ldots, is_b$, with $0 < s_k < 1$; and the strictly complex $t_1, \ldots, t_c$, with $0 < |t_l| < 1$. In addition, $w = 0$ is a zero or pole of odd order, as is implied by (16a) and (16b). Then f is given by

$$f(w) = \epsilon w^n \prod_{j=1}^{a} \left(\frac{w^2 - r_j^2}{r_j^2 w^2 - 1} \right)^{\rho_j} \prod_{k=1}^{b} \left(\frac{w^2 + s_k^2}{s_k^2 w^2 + 1} \right)^{\sigma_k} \times \\ \times \prod_{l=1}^{c} \left(\frac{(w^2 - t_l^2)(w^2 - \bar{t}_l^2)}{(t_l^2 w^2 - 1)(\bar{t}_l^2 w^2 - 1)} \right)^{\tau_l}. \tag{17}$$

Here, ρ_j is 1 or -1 according to whether r_j is a zero or a pole (note that the r_j's needn't be distinct), and similarly for σ_k and τ_l. n, an odd integer, determines the order of the zero or pole at the origin. The coefficient ϵ, given by $(-1)^a f(1)$, is equal to ± 1 (from (16a) and (16c)). It is straightforward to verify that (17) satisfies tangent boundary conditions, and therefore characterises, via (15), the radially constant, conformal, tangent unit-vector fields $\mathbf{n}$ in R for which f has a meromorphic extension to $\mathbb{C}^e$. We remark that rational functions have been used extensively as the basis for an ansatz for *skyrmions*, minimum-energy configurations of fixed baryon number (ie, degree) of localised, nonlinear $SU(2)$-valued fields in $\mathbb{R}^3$. The ansatz yields very

good descriptions of the (numerically determined) energies and topologies of the true minimisers (see, eg, [13], [14], [15]).

The values of the topological invariants can be computed in terms of the parameters of f. From (1), straightforward calculation gives $\mathbf{D} = \mathcal{A}\hat{\mathbf{r}}$, where $\mathcal{A}$, regarded as a function of w, is given by

$$\mathcal{A} = 4|f'|^2/(1+|f|^2)^2. \tag{18}$$

It follows that $\Omega^0 = \int_Q \mathcal{A}\, d^2w$. The conditions (16) above imply that $\mathcal{A}$ is invariant under $w \mapsto -w$, $w \mapsto \bar{w}$, and $w \mapsto 1/w$. Therefore, $8\Omega^0$ is given by the integral of $\mathcal{A}$ over $\mathbb{C}^e$. But this quantity is just (4π times) the degree of f, regarded (inverse stereographically) as a map from S^2 into itself. The degree of a meromorphic function is just the number of its zeros (or any other value) counted with multiplicity. Therefore,

$$\Omega^0 = \tfrac{1}{2}(|n| + 2(a+b) + 4c)\pi. \tag{19}$$

The edge orientations are easily determined from the values of f at 1, i and 0 (the images of the x, y and z-edges respectively). Let $e_x = \pm 1$ according to whether $\mathbf{n} = \pm\hat{\mathbf{x}}$ along the x-edge, and similarly for e_y and e_z. Then

$$e_x = \epsilon(-1)^a,\ e_y = \epsilon(-1)^b(-1)^{(n-1)/2},\ e_z = \operatorname{sgn} n. \tag{20}$$

The kink number k_z along the z-face can be computed from the change in phase of f along the quarter circle of $|w| = 1$ between 1 and i. The kink numbers k_x and k_y along the x and y -faces can be computed by counting zeros of f with an appropriate sign along the respective intervals $[0,1]$ and $[0,i]$. The result is

$$\begin{aligned} k_x &= -\tfrac{1}{2}(-1)^b e_y(\textstyle\sum_{k=1}^{b}(-1)^k\sigma_k + \tfrac{1}{2}(1-(-1)^b)e_z), \\ k_y &= -\tfrac{1}{2}(-1)^a e_x(\textstyle\sum_{j=1}^{a}(-1)^j\rho_j + \tfrac{1}{2}(1-(-1)^a)e_z), \\ k_z &= \tfrac{1}{4}\,(e_x e_y - n) - \tfrac{1}{2}\textstyle\sum_{j=1}^{a}\rho_j - \tfrac{1}{2}\sum_{k=1}^{b}\sigma_k - \sum_{l=1}^{c}\tau_l. \end{aligned} \tag{21}$$

As remarked above, the kink numbers and edge orientations determine the trapped areas up to an integer multiple of 4π. Moreover, trapped areas with any such multiple can be realised. For conformal configurations (17), it can be shown, using (19) – (21), that all values of the trapped area Ω^0 greater than $\Omega_{\min} = 2\pi(|k_x| + |k_y| + |k_z| + \frac{1}{4})$ can be realised. Anticonformal configurations (obtained by replacing w with $\bar{w}$) allow for all values of Ω^0 less than $-\Omega_{\min}$. Further details along with a discussion of the remaining values of Ω^0 will be given elsewhere [16].

It is possible to get better upper bounds by evaluating the integrals in (13) exactly. We do this explicitly for the configuration $f(w) = w$. We call this

configuration *unwrapped*, because it is topologically the simplest possible; its kink numbers are zero and its trapped area has the minimum allowed value. There are in fact eight distinct unwrapped configurations generated by the transformations $w \mapsto -w$, $1/w$ and $\bar{w}$. All have the same energy. For $f(w) = w$, it is readily computed that $\mathbf{D} = \mathbf{r}/r^3$. From (13), the contribution to the energy from the interior face $\{x = \frac{1}{2}L_x\}$ of R is given by

$$8KL_x \int_0^{\frac{1}{2}L_y} \int_0^{\frac{1}{2}L_z} \frac{dy\,dz}{\frac{1}{4}L_x^2 + y^2 + z^2} = \\ = 2a_{yx}a_{zx}KL_x \int_0^1 \int_0^1 \frac{u^{-\frac{1}{2}}v^{-\frac{1}{2}}}{1 + a_{yx}^2 u + a_{zx}^2 v}\,du\,dv. \quad (22)$$

The last integral may be identified with an integral representation of the Appell hypergeometric function $F_2(\alpha, \beta, \beta', \gamma, \gamma'; s, t)$ [17], with parameters $\alpha = 1$, $\beta = \beta' = \frac{1}{2}$, $\gamma = \gamma' = \frac{3}{2}$ and arguments $s = -a_{yx}^2$ and $t = -a_{zx}^2$. The integrals over the two other interior faces of R are evaluated similarly, while the integrals over the external faces vanish by tangent boundary conditions. Thus, the unwrapped energy is

$$E_0 = 8 \sum_i a_{ji}a_{ki}KL_i F_2(1, \tfrac{1}{2}, \tfrac{1}{2}, \tfrac{3}{2}, \tfrac{3}{2}, -a_{ji}^2, -a_{ki}^2), \quad (23)$$

where i runs over x, y and z, and (i, j, k) is a cyclic ordering of (x, y, z). For a cube ($L = K = 1$), this gives an upper bound of 15.3, about 20% more than $E_- = 4\pi$.

For conformal configurations other than the unwrapped ones, the energy $16K \int_{\partial R} r\mathbf{D} \cdot \mathbf{dS}$ depends on the positions r_j, s_k, t_l of the zeros and poles, and therefore can be minimised with respect to these parameters. Since $\int_{\partial R} \mathbf{D} \cdot \mathbf{dS}$ is the trapped area Ω^0, and therefore is parameter-independent, it is evident that the minimum energy is achieved by making $|\mathbf{D}|$ small at points of ∂R where r is large, and large at points where r is small. The local minima of r are just the corners of R on the x-, y- and z-edges, with projections $w = 1$, i and 0. For a cube, the corners are all equally close to the origin, and the minimum energy is approached in the singular limit in which the zeros and poles of f are made to coalesce, pairwise, at 1, i or 0 (so that, from (18), $|\mathbf{D}| = \mathcal{A}$ is made to diverge there), leaving a single zero or pole at $w = 0$. In this limit, all the topologically nontrivial behaviour (kinking and wrapping) concentrates at the edges, while away from the edges the configuration becomes unwrapped. This is reminiscent of the dipole configurations of Ref. [5]. However, for rectangular prisms, the minimum energy within a conformal family may be realised for a nonsingular configuration.

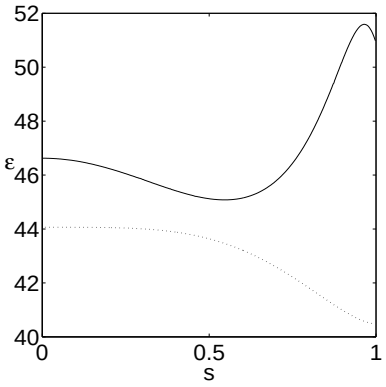


Figure 1: Scaled energy $\epsilon = E/V^{\frac{1}{3}}$ of the conformal configuration $w(w^2 + s^2)/(s^2w^2 + 1)$. Solid curve: $L_x = 20$, $L_y = 10$, $L_z = 1$. Dashed curve: $L_x = L_y = L_z = 1$.

This is illustrated in Fig. 1, which shows the energy (scaled by the cube root of the volume) of the configuration $f(w) = w(w^2 + s^2)/(s^2w^2 + 1)$. For a cube (dashed curve), the energy approaches a minimum as s approaches 1, corresponding to a configuration which is singular along the y-edge. For $L_x = 20$, $L_y = 10$, $L_z = 1$ (solid curve), the energy has a minimum for s between 0 and 1, corresponding to a smooth configuration. (The nontrivial kink number $|k_z| = 1$ rules out conformal deformations of f to a configuration which is singular along the shortest z-edge.) Numerical solutions of the Euler-Lagrange equations (4) exhibit the same transition [16]. One would expect to observe the smooth configurations but not necessarily the singular ones; in the vicinity of such an edge singularity, the liquid crystal could melt, losing orientational order, and then relax to an unwrapped state.

The preceding analysis indicates that the stability of topologically nontrivial tangent director configurations in rectangular prisms depends on the (purely geometrical) aspect ratios, a phenomenon which will be the subject of further investigation.

AM was supported by an EPSRC/Hewlett-Packard Industrial CASE Studentship. MZ was partially supported by a grant from the Nuffield Foundation. We thank CJ Newton and A Geisow for stimulating our interest in this area.

References

[1] P.-G. de Gennes and J. Prost. *The physics of liquid crystals*. Oxford University Press, 2nd edition, 1995.

[2] N.D. Mermin. The topological theory of defects in ordered media. *Rev. Mod. Phys.*, 51C:591–651, 1979.

[3] M. Kléman. *Points, Lines and Walls*. John Wiley and Sons, Chichester, 1983.

[4] O.D. Lavrentovich. Topological defects in dispersed liquid crystals, or words and worlds around liquid crystal drops. *Liquid crystals*, 24:117–125, 1998.

[5] H. Brezis, J.-M. Coron, and E.H. Lieb. Harmonic maps with defects. *Comm. Math. Phys.*, 107:649–705, 1986.

[6] C.D. Santangelo and R.D. Kamien. Bogolmol'nyi, Prasad, and Sommerfield configurations in smectics. *Phys. Rev. Lett.*, 91:5506–5509, 2003.

[7] G. Tóth, C. Deniston, and J.M. Yeomans. Hydrodynamics of topological defects in nematic liquid crystals. *Phys. Rev. Lett.*, 88:5504, 2002.

[8] P. Patrício, M.M. Telo da Gama, and S. Dietrich. Geometrically-controlled twist transitions in nematic cells. *Phys. Rev. Lett.*, 88:5502–5505, 2002.

[9] C.J.P. Newton and T.P. Spiller. Bistable nematic liquid crystal device modelling. In *Proc. 17th IDRC (SID)*, page 13, 1997.

[10] S. Kitson and A. Geisow. Controllable alignment of nematic liquid crystals around microscopic posts: Stabilization of multiple states. *Appl. Phys. Lett.*, 80:3635 – 3637, 2002.

[11] J.M. Robbins and M. Zyskin. math-ph/0402025, to be published in *J. Phys. A*.

[12] A. Majumdar, J.M. Robbins, and M. Zyskin. math-ph/0406005, to be published in *Lett. Math. Phys.*

[13] C.J. Houghton, N.S. Manton, and P.M. Sutcliffe. Rational maps, monopoles and skyrmions. *Nucl. Phys. B*, 510:507, 1998.

[14] R. Battye and P. Sutcliffe. Skyrmions, fullerenes and rational maps. *Rev. Math. Phys.*, 14:29–86, 2002.

[15] T. Ioannidou, B. Kleihaus, and W. Zakrzewski. An improved harmonic map ansatz. *Phys.Lett. B*, 597:346–351, 2004.

[16] A. Majumdar, J.M. Robbins, and M. Zyskin. in preparation.

[17] I.S. Gradshteyn and I.M. Ryzhik. *Tables of Integrals, Series and Products*. Academic Press, 1980.